

## **Field Measurements of the Total and Spectral Albedo of Snow and Ice in Dronning Maud Land, Antarctica**

*Kai Rasmus*

Department of Physical Sciences, Division of Geophysics, P.O. Box 64, FI-00014 University of Helsinki

(Received: September 2002; Accepted: May 2006)

### *Abstract*

*Variabilities in the spectral and total (between 300-3000 nm) albedo of snow were studied in the Dronning Maud Land region of Antarctica during the austral summers of 1999/2000 and 2000/2001. The measurement area consisted of a traverse going inland from the coast via the Finnish Antarctic research station Aboa, and the vicinity of the South African Antarctic station SANAE 4. The results show that midday mean total albedos for snow were between 0.83, for clear skies, and 0.86, for overcast skies, at Aboa and between 0.81 and 0.83 for SANAE 4. The variations in the spectral albedos could be explained by differences in cloud cover. The mean spectral albedos at Aboa and SANAE 4 were very close to each other. The near infrared (700-3000 nm) albedo related well to the total albedo and the ultraviolet (300-400 nm) albedo related well to the visible (400-700 nm) albedo. Other narrowband albedos did not correlate well with each other.*

*Key words: albedo, spectral albedo, snow, blue-ice, Antarctica*

### *1. Introduction*

A unique feature of both the Greenland and Antarctic ice sheets is that the annual mean net radiation at their surface is negative. This is compensated by a sensible heat flux from the air, which introduces additional cooling in the lower atmosphere. This is especially important in the katabatic wind zone, where increased surface cooling increases the sensible heat transport. This close interaction between the radiation climate and boundary layer dynamics makes the large ice sheets extraordinary components of the global climate system (*Van den Broeke, 2004*). In Antarctica, the surface solar radiation budget is dominated by the high albedo of the snow cover, which is between 0.8-0.9 for dry snow (*Wendler and Kelley, 1988; Orsini et al., 2000*) in clear sky conditions. For wet snow, which can occur near the coast of Antarctica (*Kärkäs et al., 2002*), the albedo is between 0.7-0.8. When the albedo is high, even small changes cause large relative changes in the amount of radiation absorbed: a decrease from 0.9 to 0.8 doubles the level. Due to the size of the Antarctic ice sheet, and its importance in the global climate system, it is important also to know the spatial variations in albedo.

Normally only one dry snow albedo value is used in climate modelling and usually the measured parameter available is a narrowband albedo. The physical properties of snow that affect the albedo in the near-infrared band are different to the ones that affect the albedo in the visible band causing a difference in the ratios of narrowband-to-total albedo. It is therefore important to know the spectral distribution of the albedo. So far, most albedo studies in Antarctica have been either at point locations or on traverses across the polar plateau at a high elevation where the snow conditions are drier than in the coastal zone. There exists a need for more measurements of albedo in different areas of Antarctica.

The albedo of snow is mostly affected by the back scattering of light from ice grains, increasing with decreasing size of grains. The presence of liquid water in the ice grain matrix causes an increase in the optically significant grain size of snow as far as scattering is concerned because the water surrounds the ice grains, and water and ice have a very similar real index of refraction. Liquid water absorbs radiation slightly better than ice causing a slight decrease in the albedo (*Warren, 1982*).

Impurities, such as soot or dust, within the snow absorb radiation more efficiently than the ice in the snow grains, thus lowering the albedo of the snow cover. *Warren and Clarke (1990)* found that very small concentrations of soot that are invisible to the naked eye decrease the albedo of snow. They concluded however, that even in the exhaust plume of a large inland station the concentration of soot (3 ng/g) is too small to affect the albedo significantly. Therefore, the albedo measured at such a location is representative of the surrounding ice sheet. Closer to the coast, dust from mountain ranges and absorbing aerosols and marine hydrosols can lower the albedo of the snow cover.

Over a uniform snow cover, the albedo increases with decreasing solar elevation angle (*Pirazzini, 2004*). *Wendler and Kelly (1988)* found that the dependency on solar elevation was small for solar elevations above 12°. Cloud cover absorbs infrared radiation, which would normally be absorbed by the snow cover, causing an increase in the albedo of snow. Cloud cover affects the spectral albedo by changing the angular distribution of the incoming solar radiation (*Warren, 1982*). When surface roughness, such as sastrugi, is present, the diurnal variation of the albedo becomes asymmetrical with regard to the highest solar elevation. At low solar elevation angles when the sun shines from behind the sastrugi, the surface can appear relatively dark producing a low albedo.

The main objective of this present study was to examine the spatial variability of the spectral and total albedo in the coastal region below 1100m above sea level (asl) in the Dronning Maud Land area. The measurements were made along the same traverse and during the same time as the snow measurements of *Kärkäs et al. (2002)*. The goals were to find out whether the variations in the physical properties of the snow in different snow regions are optically significant or whether ambient conditions (cloud cover and solar elevation) dominate the variations, and to find out how the spectral and total albedos relate to each other.

Measurements of total and spectral albedo of snow were made on a traverse going inland from the coast via the Finnish research station Aboa (73° 03.1' S, 013° 27.7' W) and in the vicinity of the South African research station SANAE 4 (71° 40.0' S, 002° 51.0' W). The measurements were made during the austral summers of 1999/2000 and 2000/2001 as part of the FINNARP 99 and FINNARP 2000 expeditions.

The physical properties of snow, mainly the density, stratigraphy and wetness, have been used to divide the traverse into 4 distinct snow zones (*Kärkäs et al.*, 2002). However, the main optically significant physical properties of snow show only small variations on the Antarctic ice sheet, and so variations observed in the albedo observations must be mainly due to variations in ambient conditions.

The results show that the spectral albedo of snow is high with very little wavelength dependence between 300 and 1100 nm. The observed spatial variability can be explained with the variations in cloudiness. The snow albedos were significantly different from the albedos of blue ice and superimposed ice, which is ice that has gone through one or more melt-freeze cycles.

## 2. Materials and methods

### 2.1 Definitions

The spectral albedo,  $\alpha(\lambda)$ , is defined as the ratio of upwelling ( $E_u$ ) to downwelling ( $E_d$ ) spectral irradiance:

$$\alpha(\lambda) \equiv \frac{E_u(\lambda)}{E_d(\lambda)} \quad (1)$$

where  $\lambda$  is the wavelength. This parameter is sometimes called the spectral reflectance but the nomenclature used in this study is similar to e.g. *Grenfell and Perovich* (2004). Narrowband albedos,  $\alpha_{nb}$ , can be obtained from Eq. (1) by integrating the upwelling and downwelling irradiances over a closed wavelength range  $[\lambda_1, \lambda_2]$ :

$$\alpha_{nb}[\lambda_1, \lambda_2] = \frac{\int_{\lambda_1}^{\lambda_2} \alpha(\lambda) E_d(\lambda) d\lambda}{\int_{\lambda_1}^{\lambda_2} E_d(\lambda) d\lambda} \quad (2)$$

In this study, the term total albedo will be used when the integration band is the same as pyranometers measure (i.e. between 300 and 3000 nm). The total albedo is sometimes referred to as the broadband albedo (e.g., *Greuell et al.*, 2002).

## 2.2 Description of measurement area

Measurements of spectral and total albedos together with measurements of snow properties were made in 1999/2000 along a traverse going inland from the coast via Aboa. The Aboa traverse included measurements on Högisen ice dome (73° 26.3' S, 014° 26.7' W). During the following summer, similar measurements were made in the vicinity of SANAE 4. Blue ice areas close to SANAE 4, Aboa and an area close to the Heimefrontfjella mountain range were measured. The blue ice area at SANAE 4 included some superimposed ice. The dates and co-ordinates of the measurement sites are given in Table 1. A map of the measurement area is shown in Fig. 1.

Table 1. List of points on the Aboa transect and SANAE 4 where the albedo was measured with the LI1800UW and EP16 during the 1999/2000 season.

Name	Date	Time	Cloud	Solar elevation	Latitude	Longitude
OG6	24 Dec. 99	14:15	7	36.5	73° 02.0' S	013° 19.5' W
IS2	25 Dec. 99	18:00	7	21.2	72° 45.2' S	014° 18.3' W
IS1	26 Dec. 99	12:45	7	40.5	72° 40.0' S	016° 42.0' W
OG3	02 Jan. 00	13:10	1	39.6	72° 57.9' S	013° 34.9' W
Aboa blue ice	06 Jan. 00	12:50	0	38.9	73° 03.1' S	013° 27.7' W
IG7	08 Jan. 00	16:05	2	29.0	73° 12.5' S	013° 13.0' W
IG4	10 Jan. 00	11:42	7	38.3	73° 27.4' S	012° 33.4' W
IG9	15 Jan. 00	21:00	4	9.0	74° 28.7' S	011° 33.0' W
IG5	16 Jan. 00	12:00	8	36.5	74° 00.8' S	012° 01.0' W
H8 (Högisen)	23 Jan. 00	15:03	7	30.4	73° 26.3' S	014° 26.7' W
SANAE 4	Dec. 00- Jan. 01				71° 40.0' S	002° 51.0' W

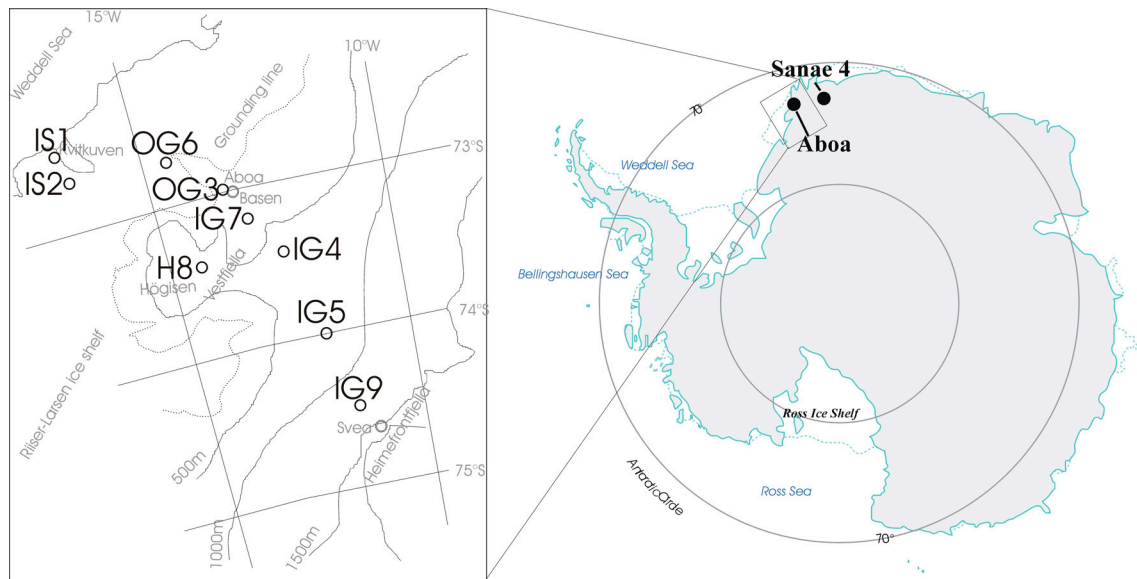


Fig. 1. Map showing the locations of the measurement areas and the locations of the measurement points on the Aboa traverse. The coastline and altitude contours are marked with solid lines and the dotted line indicates the location of the grounding line, which is where the ice sheet meets bedrock.

The Aboa traverse is characterised by high mountain ranges, called Vestfjella and Heimefrontfjella that obstruct the ice flow. The Heimefrontfjella mountain range especially causes a sudden transition from the polar plateau to the coastal region. The glacier is mainly unobstructed between the ranges. *Van den Broeke et al.* (1999) deduced that katabatic winds are active there by making measurements of the potential temperature, near-surface firn density and accumulation. The winds were from a South-Easterly direction.

*Kärkäs et al.* (2002) identified four definite snow zones in this section based on the physical properties of the snow cover. On the ice shelf (IS) the snow grain size is approximately a millimetre and the mean density is  $427 \text{ kg m}^{-3}$ . Due to melting, the snow wetness can become significant. Inland of the ice shelf the snow is dense (between  $415\text{--}445 \text{ kg m}^{-3}$ ) and hard with only some melting occurring. This region will be referred to as the outer glacier (OG). Above the grounding line and inland of the Vestfjella mountain range, the snow is not as hard and dense as in the previous zone (density  $390\text{--}430 \text{ kg m}^{-3}$ ). This region will be referred to as the inner glacier (IG). On the local ice domes the snow surface is smoother and the snow has a lower density ( $340 \text{ kg m}^{-3}$ ), which is an indication of locally reduced speeds in the katabatic wind on the domes. The area surrounding SANAE 4, which is located on Vesleskarvet nunatak, is punctured by nunataks in many places and the mountains are not only in distinct ranges.

Snow-free regions of Antarctica are either exposed rocks, nunataks, or ice. Snow-free ice areas that do not suffer surface melt but are kept snow-free due to wind action are called blue-ice areas. They have a total albedo of 0.5-0.6. According to *Bintanja* (1999), blue-ice areas are usually found only above 2000 m asl. Lower altitude snow-free ice areas are also blue but they often include internal melt water pools and suffer surface melt.

There is less backscattering in ice than in snow leading to a higher probability of a photon being absorbed before it is able to escape from the ice. The absorption and scattering spectra of pure ice are very close to those of liquid water: absorption has a minimum at 500 nm and strongly increases towards red and near infrared wavelengths, while scattering decreases by wavelength to the power of  $-4$ . This means that ice appears blue, since red wavelengths are absorbed by the ice. Air bubbles in ice cause light to be scattered more in directions away from the forward direction and therefore the higher the content of air bubbles in the ice, the whiter the ice appears and the higher its albedo becomes. Superimposed ice, which forms when melting snow and ice refreezes, has a large air bubble content. This means that it is not as white as snow but not as blue as ice.

### 2.3 Measurements

Spectral irradiance measurements were made using a Li-Cor LI1800UW spectroradiometer with a remote cosine corrector mounted on a pole with the sensor head 30cm above the snow cover. The length of the fibre-optic cable used in the remote sensor limited the distance between the sensor head and the surface. Downwelling

irradiance was measured first and then the upwelling irradiance was measured. The instrument has a spectral resolution of 6 nm. For this study, the radiation spectrum was scanned from 300 to 1100 nm, which took about 45s to complete. The length of the integration time becomes a problem in highly variable light conditions but measurements were made in relatively stable sky conditions with the sun either totally behind or uncovered by cloud. The instrument is accurate to  $\pm 0.1 \text{ Wm}^{-2} \text{ nm}^{-1}$ , which produces an error of  $\pm 0.001$  in the spectral albedo values for snow.

The LI1800 instrument measures upwelling and downwelling irradiance directly, eliminating the need for assumptions to be made of the surface, or of reference measurements over a lambertian reflector, before the albedo can be calculated.

A Middleton EP-16 pyranoalbedometer system was used to make total albedo measurements. This system measured downwelling and upwelling irradiances simultaneously over the 300 to 3000 nm band. The instrument was mounted on a rod, which was clamped to a tripod. This set-up placed the sensor head 1 m above the ground. The sensors were calibrated in March 1999. The calibration accuracy of the EP-16 pyranometers is 3% of the absolute irradiance. The instrument was levelled with a spirit level located on the instrument housing to keep the tilt error to a minimum. Absolute tilt error was found to be 0.02 (for 1 degree of tilt) in albedo over a terrain with sastruga of approximately 10cm amplitude and a wavelength of 1m. Over this kind of surface, the error caused by instrument tilt was estimated to be 3% of irradiance per degree of tilt using measured data. The accuracy of the EP-16 was checked over a rocky surface in the vicinity of Aboa station. It was assumed that the optical properties of the rock do not change during the measurement. A 120 min measurement produced a value of 0.11 for the albedo of the rock with a standard deviation of 0.005. The number of albedo measurements was 251.

The snow properties at SANAE 4 were measured from shallow snow pits. The density was measured by taking 0.2 l of snow with a metal cylinder and weighing the sample with an electronic scale. The accuracy of the volume measurement was about  $\pm 0.01$  l and the accuracy of the weight measurement was  $\pm 1$  g. For a typical sample weight of 60 g, this produces an error of  $\pm 10 \text{ kgm}^{-3}$  in the density. The grain sizes have been measured by comparing snow grains visually with a millimetre scale, which was a relatively inaccurate method. A description of the methods used to make the Aboa snow measurements can be found in *Kärkäs et al. (2002)*.

### 3. *Measurement results*

#### 3.1 *Snow conditions*

The surface snow properties for SANAE 4 are shown in Table 2 together with the total albedos. At SANAE 4, the surface snow density remained between 403 and  $465 \text{ kgm}^{-3}$  throughout the measurement period and the surface grain size was  $0.5 \pm 0.4$  mm. The reader is referred to *Kärkäs et al. (2002)* for a detailed description of the surface properties along the Aboa transect. The following mean maximum diameter

results for the different snow zones were found: 1.50 mm (2 points) for the ice shelf, 1.25 mm (2 points) for the outer glacier and 1.26 mm (3 points) for the inner glacier. Högisén crystals showed a maximum grain diameter of 0.8 mm but they were measured several weeks before the spectral albedo measurement was made there.

When divided into the snow zones obtained by *Kärkäs et al.* (2002), points IS1 and IS2 fall into the ice shelf zone, points OG3 and OG6 fall into the outer glacier and points IG4, IG5, IG7 and IG9 into the inner glacier zone.

Table 2. Snow properties in the SANAE 4 area together with the total albedo. The grain size was always approximately 0.5 mm. The grains were rounded.

Date	Density surface (kgm <sup>-3</sup> )	Temp gradient surface (°C m <sup>-1</sup> )	Temp gradient 50cm (°C m <sup>-1</sup> )	Cloud	Albedo (12:00)
27 Dec 2000	454	-34	-2	1	
3 Jan 2001	439*	-	-	8	0.83
8 Jan 2001	450	-10	-4		
15 Jan 2001	403	-50	-6		0.81
21 Jan 2001	465**	-	-	3	0.82
26 Jan 2001	454	-30	-2		

\* mean of 3 measurements  
\*\* mean of 4 measurements

### 3.2 Albedo results

Mean spectral albedos for five different types of snow and ice are shown in Fig. 2. The result for snow from the Aboa dataset and the SANAE 4 data are seen to be almost identical. Blue ice shows the lowest values and the superimposed ice shows values in between snow and ice. The SANAE 4 blue ice has lower values in the red and infrared than the Aboa blue ice. The spectral albedos measured at Aboa and SANAE 4 are shown in Fig. 3 grouped into three cloudiness groups. Cloud fractions 1/8 and 2/8 were considered to represent totally clear skies and cloud fractions 7/8 and 8/8 totally overcast. The spectra have been averaged into the three groups in the lower panel of Fig. 3. The curves measured under almost overcast skies at high solar elevations show the highest albedo values in the visible band. At 1034 nm, the curves with a slightly lower sun angle show a higher albedo value. The albedos measured during a lower cloud fraction show smaller values across the spectrum.

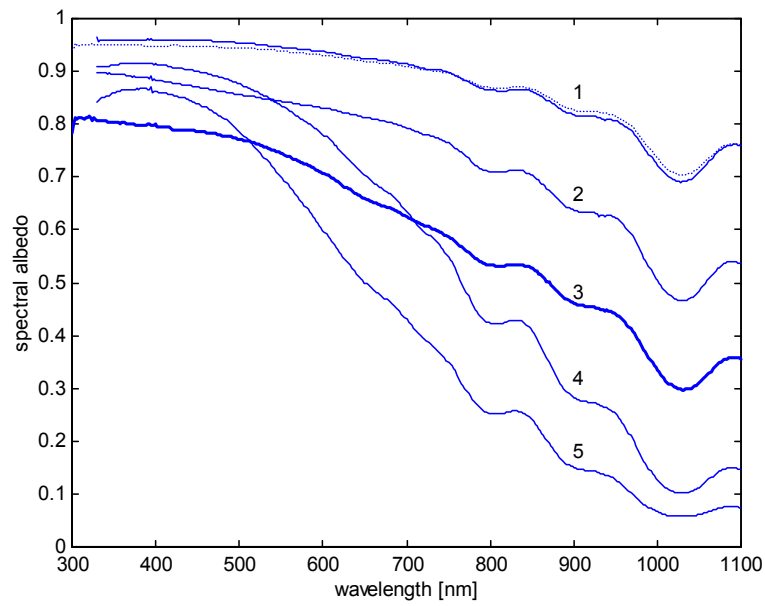


Fig. 2. Mean spectral albedos from the two expeditions: 1- mean spectral albedo Aboa dataset ( $\_$ ) and SANAE 4 data ( $--$ ), 2- superimposed ice from SANAE 4, 3- Blue ice from near Aboa. 4 and 5- Blue ice from SANAE 4.

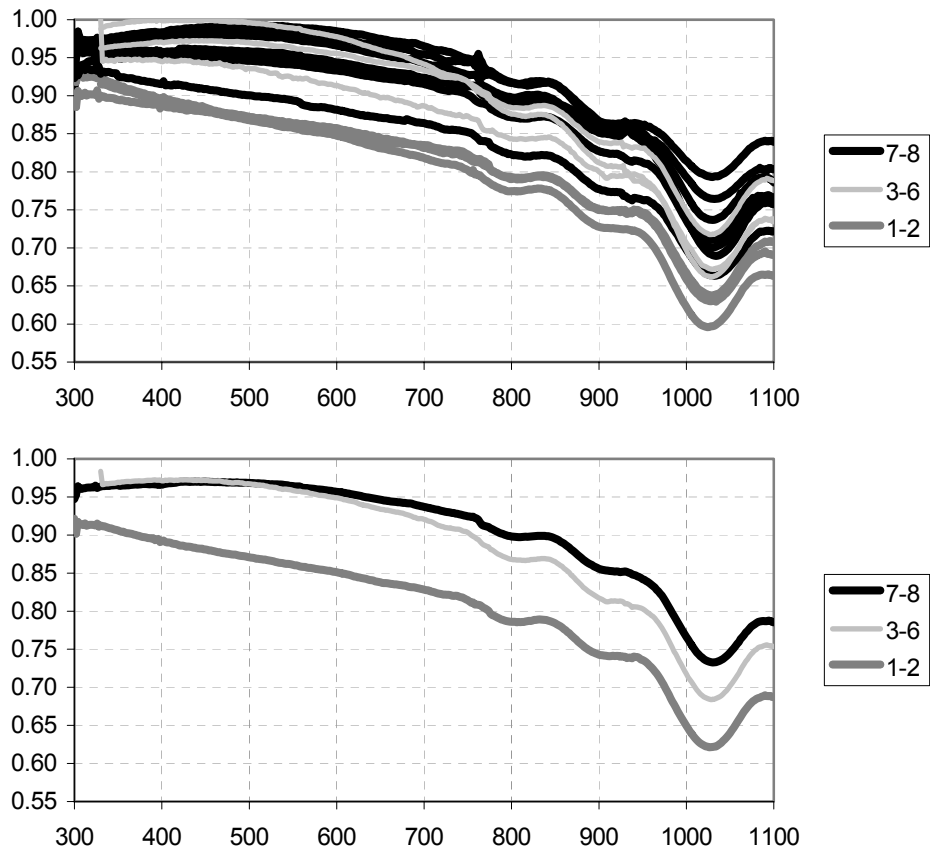


Fig. 3. Spectral albedos for snow under different amounts of cloud. All of the spectra are shown in the upper panel and they have been averaged into the three groups in the bottom panel.

The total albedo for IG4 is shown in Fig. 4. The cloud cover was between 5/8 and 8/8 during the 4 hour duration of this measurement. The afternoon albedo is 0.04 lower than the morning albedo. This change coincides with a rapid increase in cloudiness with the sun coming out from behind cloud during noon.

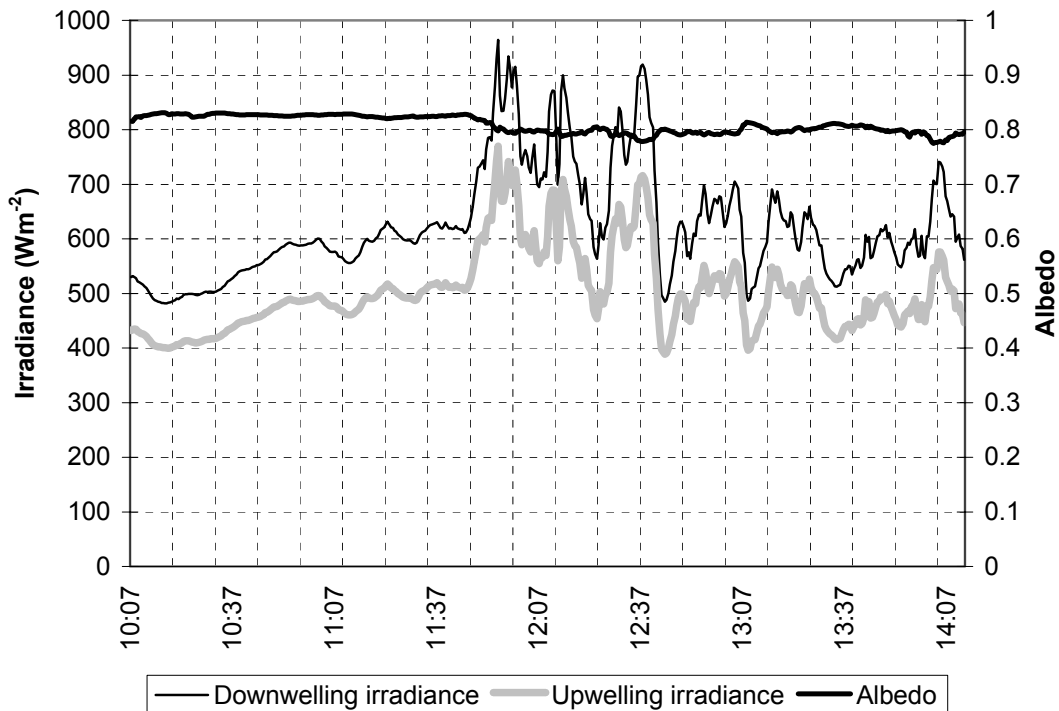


Fig. 4. The measured total albedo at IG4 together with the measured integrated downwelling and upwelling irradiances.

The mean total albedos on the Aboa traverse were 0.859 for the IS (2 measurement points, cloud fraction 8/8 and 0.002 standard deviation), 0.849 (3 points, cloud fraction variable and 0.040 standard deviation) for the OG and 0.817 (3 points, cloud fraction between 2/8 and 8/8 and 0.016 standard deviation) for the IG. No total albedo measurements were made on the snow domes. The small amount of data does not allow adequate statistical treatment.

### 3.3 Relations between narrowband and total albedos

The narrowband albedos are shown in Fig. 5 plotted against the solar elevation. They show a weak positive linear dependence on solar elevation. In the 300-400 nm band the coefficient of determination ( $R^2$ ) is 0.80 ( $N=8$ ). The different narrowband albedos for snow follow a pattern in which the 300-400 nm band has the highest albedo and the 700-1100 nm band has the lowest albedo, with the visible band (between 400 and 700 nm) having an albedo between these two. Only one point showed a different pattern but at this point, the solar elevation was less than 10 degrees. Blue ice and superimposed ice follow the same pattern but the differences between the highest and lowest values are larger.

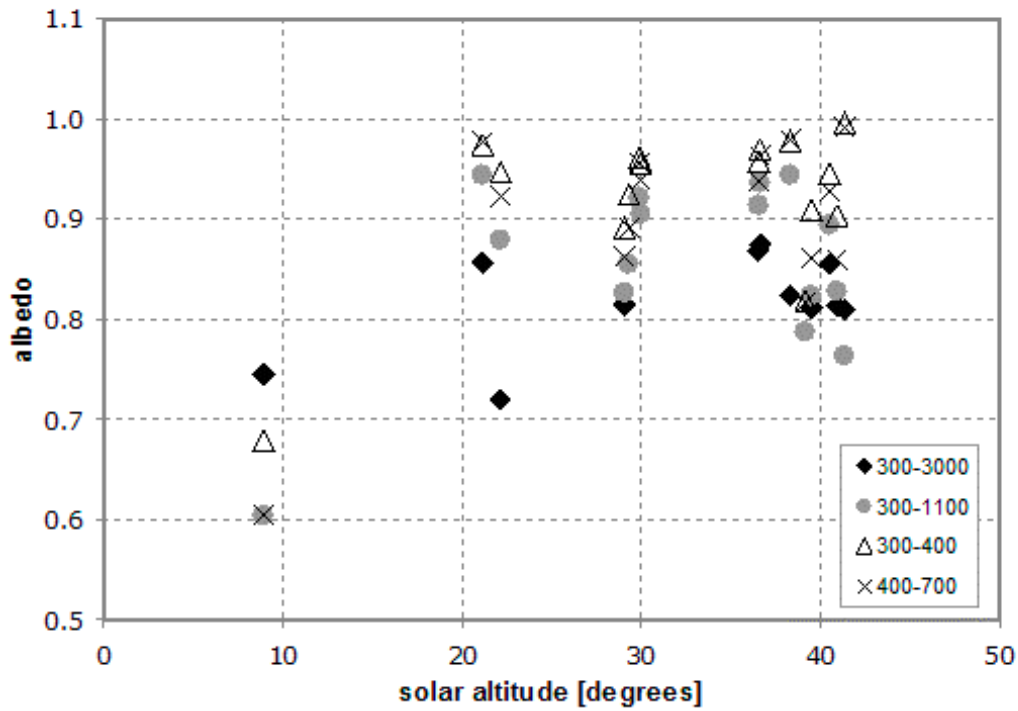


Fig. 5. The narrowband albedos plotted against the solar elevation.

The narrowband albedos for the 300-400 nm band and the 700-3000 nm band are plotted against the total albedo (300-3000 nm) in Fig. 6. The regression between the 300-400 nm band and the 300-3000 nm band was poor but between the 700-3000 and 300-3000 nm bands, the coefficient of determination ( $R^2$ ) was 0.71. The linear fit produced the following equation:

$$\alpha_{700-3000} = 1.66\alpha_{300-3000} - 0.64 \quad (3)$$

The regressions between the visible and ultraviolet bands and the 300-3000 nm band were poor ( $R^2=0.07$  and  $R^2=0.05$  respectively). However, the ultraviolet band albedo and the visible band gave the following equation:

$$\alpha_{UV} = 0.68\alpha_{VIS} - 0.31 \quad (4)$$

The coefficient of determination for Eq. (4) is 0.85. From these equations it can be seen that different narrowband albedos that are hard to measure can be calculated from albedo measurements that are made frequently.

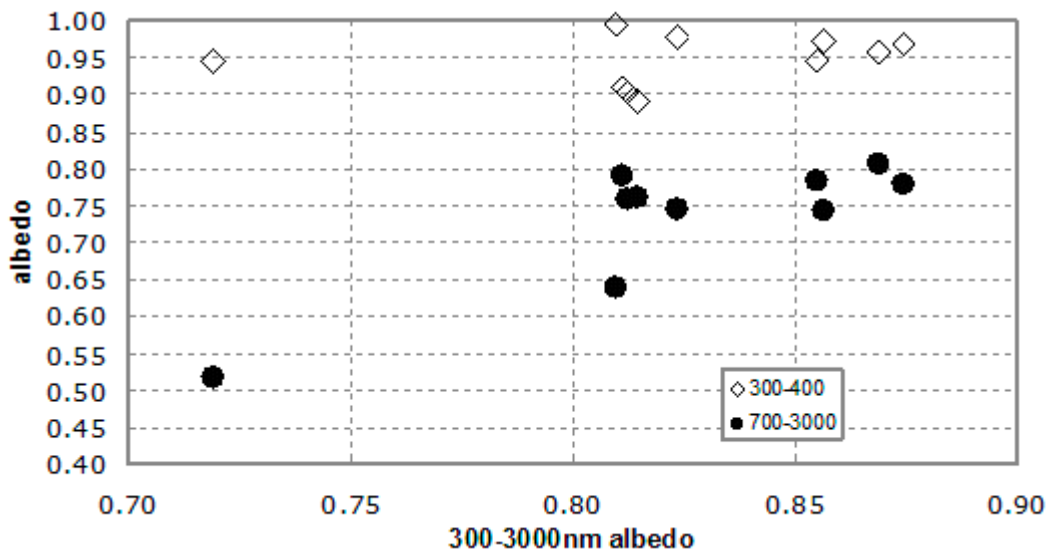


Fig. 6. Albedos for 300-400nm and 700-3000nm plotted against the total (300-3000) nm albedo.

### 3.6 LANDSAT band ratios

Landsat represents the longest continuously acquired space borne remote sensing data. It has been used for the remote sensing of continental ice sheets and Antarctica (e.g. *Reijmer et al.*, 2001). The Thematic Mapper (TM) has 3 bands in the visible wavelengths: band 1 in the blue, band 2 in the green and band 3 in the red part of the visible spectrum. It has 1 band in the near infrared. Snow and ice reflect differently in the green part of the spectrum but they have similar reflectance characteristics in the near infrared. By taking the ratio of band 4 (which is from 760-900 nm) and band 2 (520 to 600 nm), the different glacier facies (snow, blue-ice and superimposed ice) can be mapped. The TM band 4 to band 2 ratios (TM4 / TM2) for the Aboa and SANAE 4 datasets are shown in Fig. 7 plotted against the solar elevation. The figure shows that the albedo band ratios over snow and blue ice are almost independent of the solar elevation. Band ratios are normally interesting only for clear skies but no cloud cover restrictions were applied to the analysis due to the limited amount of data. The result means that the band ratio can be used for a surface classification even at low solar elevations. This comes from the fact that the reflectance into the zenith direction has a similar dependence on the solar elevation in the green and near infrared parts of the spectrum.

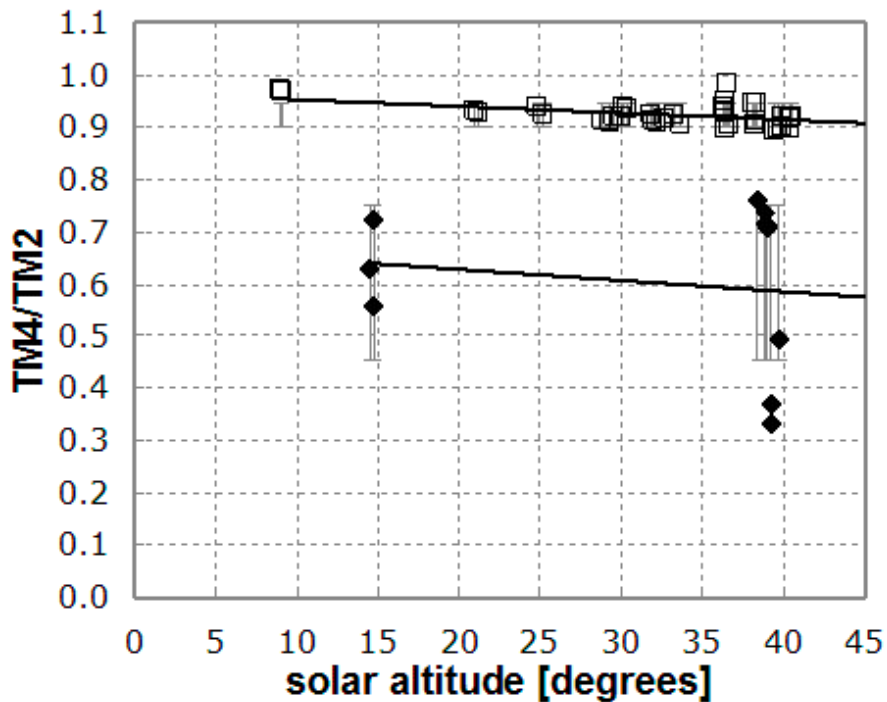


Fig. 7. The TM band ratios for the Aboa and SANAE 4 datasets. Open squares are snow and filled in diamonds are blue ice. The error bars are 1 standard deviation away from the mean.

#### 4. Discussion

##### 4.1 Spectral and total albedos

*Kärkäs et al.* (2005) report that the snow grain size distribution over the Aboa-traverse for the Austral summers of 1999/2000, 2000/2001 and 2003/2004 show a mean of 1.3 mm with a standard deviation of 0.8mm. The median value was found to be 1.0 mm. *Gay et al.* (2002) report mean convex radii of between 0.1-0.2 mm for the inner Antarctic ice sheet. The mean convex radius seems to be almost an order of magnitude smaller than the grain size reported by *Kärkäs et al.* (2005), but they took the largest grain diameter, which is almost two times as large as the mean convex radius of a grain. The mean convex radius is a measure of what size spheres could fit in the snow grains. The SANAE 4 measurements showed the grain size to be only approximately 0.5 mm. This grain size (largest diameter) range would produce albedos within 0.02 of each other in the visible wavelengths and within 0.13 of each other in the near infrared as calculated using the model by *Wiscombe and Warren* (1980). They have shown that changes in density are not major contributors to albedo variations but variations in grain size are. The grain size range alone is not enough to explain the variation in albedo as modelled by *Wiscombe and Warren* (1980). Measurements of impurities were not made but their effect is assumed small.

The mean spectral albedos for snow from the Aboa traverse and from SANAE 4 showed values of 0.95 in the visible band with small wavelength dependence. After 700 nm, the wavelength dependence increased and at 1034 nm, the albedos dipped to 0.70. The spectra were found to be statistically insignificantly different with a correlation coefficient of 0.9956. The variations due to ambient conditions seem to outweigh the spatial variations. More measurements of the spatial albedo variations are required to be sure of this. These should be of either longer duration at each measurement point or at many points simultaneously to minimize the effects of varying ambient conditions.

Overcast and partly cloudy albedo cases showed values that were 0.1 higher, between 400 and 700 nm, than the clear sky or almost clear sky cases. At higher wavelengths, the partly cloudy cases showed slightly lower values than the overcast cases.

The decrease in total albedo in the morning and evening seen in Fig. 4 coincides with an increase in the irradiance levels due to a decrease in cloud fraction from overcast to partly cloudy. The fact that cloudiness has an increasing effect on the total albedo (e.g. *Wendler and Kelley, 1988; Pirazzini, 2004*) would explain this albedo decrease. Even though the snow grains begin to melt quickly when the sun starts to shine, the metamorphism is not fast enough to explain the total coincidence in albedo with the increase in radiation. Even though there are large fluctuations in the incoming irradiance in the partly cloudy conditions, the albedo remains relatively stable.

#### 4.2 *Glacier facies*

The main differences between the spectral albedos of the Aboa and SANAE 4 blue ice areas come from the difference in texture between the two areas. At Aboa, the ice surface experiences continuous melt-freeze cycles producing a grainy structure with many boundaries that scatter light in all directions. The blue-ice area at SANAE 4 is subject to much less surface melting making it clearer with crystal boundaries invisible to the naked eye. This means that the scattering is mainly in the forward direction with less chance of escape for the scattered photon.

Snow and superimposed ice both contain many grain boundaries and air bubbles that act as scatterers for light. The grain sizes are larger in superimposed ice and therefore the albedo is lower than in snow, but higher than in bubble free blue ice. Superimposed ice has a clearly different spectral signature from that of either blue ice or snow if the whole spectrum is taken into account.

It is possible to classify the surface type into at least snow and blue ice using the TM4 / TM2 band ratio. The surfaces can be classified using classification boundaries [0.90, 0.98] for snow and [0.33, 0.76] for blue ice. Only two measurements of superimposed ice were made. The values obtained were 0.83 and 0.84 with a solar angle of 38.9°. Superimposed ice has a band ratio less than snow but higher than blue ice but it can be classified as either snow or blue-ice depending on its bubble content and therefore its likeness to snow. More measurements of superimposed ice are needed to create accurate classification boundaries for it.

### 4.3 Comparisons with other measurements

Albedo studies have been made in several regions of Antarctica. In Dronning Maud Land *Liljequist* (1956) made pioneering work at Maudheim (71° 03' S, 10° 56' W) during the Norwegian-British-Swedish Antarctic expedition of 1949-52. He found the mean total albedo of the snow cover under dense overcast clouds in situations with no drifting snow to be 0.895 at the end of the year between September and November, and dropping to 0.877 during the months of January-March. Under clear skies, he found the total albedo to vary with solar elevation being 0.83 at 13° solar elevation and dropping to below 0.80 when the solar elevation became higher than 40°. The overcast and clear sky total albedos obtained in this study were slightly higher than albedos obtained by *Liljequist* (1956) on Maudheim. The measurement site at Maudheim was situated on the ice shelf very close to the open sea, which will have had an influence on the snow cover and the amount of downwelling irradiance. The values obtained in this study at the lowest solar elevations contain the largest uncertainties. If these values are disregarded then the albedo shows a decrease with increasing solar elevation.

The total overcast albedo in Antarctica in January has been reported by *Liljequist* (1956) at Maudheim, by *Hoinkes* (1961) at Byrd Station, by *Carroll and Fitch* (1981) at the South Pole, by *Wendler and Kelly* (1988) in Terre Adelie, by *Grenfell et al.* (1994) at the South Pole and at Vostok, by *Bintanja and Van den Broeke* (1995) and *Reijmer et al.* (2001) at Svea, and by *Mishra* (1999) on the Princess Astrid Coast. *Pirazzini* (2004) reports measurements from Neumeyer, Reves Neve, Dome Concordia and Hell's gate. The measurements for all of the authors together with the measurements from this study are shown in Fig. 8. A slight decreasing trend is visible (-0.0014 per year) but because of the limited number of data points ( $N=14$ ,  $R^2=0.63$ ), the conclusion that the overcast total albedo has decreased during the years needs to be made with a certain amount of caution. The values in this study made at Aboa are the highest values obtained during the 1990-2001 period but the SANAE 4 measurements are more in line with the other measurements.

*Reijmer et al.* (2001) have found the total albedos for blue ice and snow at two points in the Heimefrontfjella region of Dronning Maud Land, to be 0.60 and 0.78. They also found the narrowband albedos in TM bands 2 and 4 to be 0.97 and 0.86 respectively for snow and 0.87 and 0.51 for blue ice. Their measurements were made in a location (74° 35' S, 11° 13' W) surrounded by mountains. The total albedos near Aboa are slightly higher.

*Carroll and Fitch* (1981) and *Wendler and Kelly* (1988) both obtained total albedo values that were 0.83 for dry snow for clear conditions and over 0.90 for overcast conditions. The values in the present study are slightly lower. The snow measurements show that their study was made in an area that was mainly on the border of the dry snow zone at a high altitude.

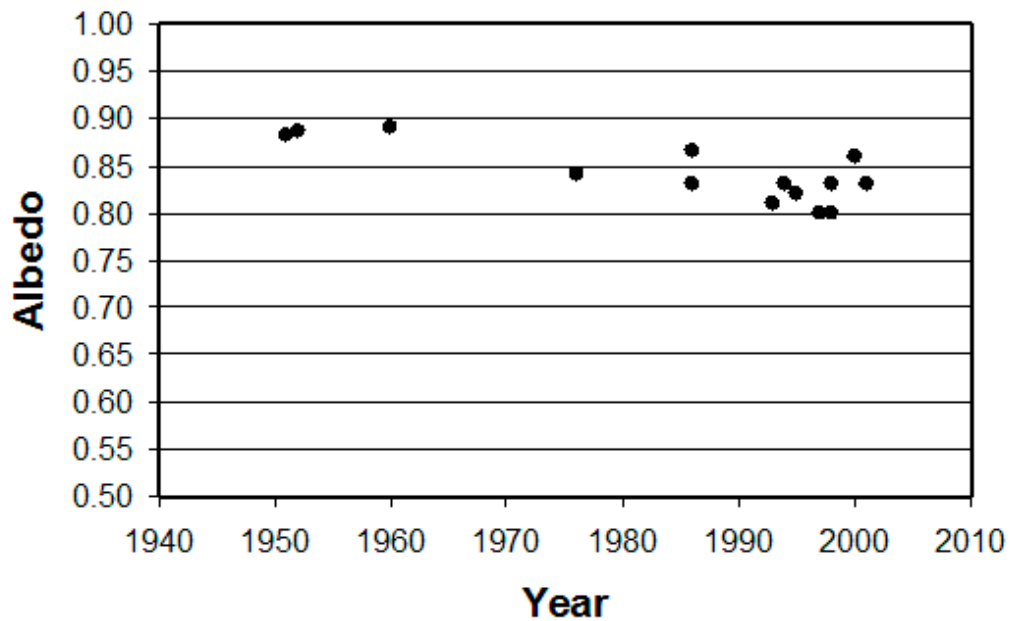


Fig. 8. The overcast total albedos measured in January from different authors.

*Casacchia et al.* (2002) have studied the spectral albedo of snow compared to the physical properties of the snow at the Italian Antarctic research station at Terra Nova Bay ( $74^{\circ} 41' S$ ,  $164^{\circ} 07' E$ ). They found that a detailed characterisation of snow metamorphism is important to describe the variation in the spectral albedo. *Orsini et al.* (2000) studied the albedo of a sastrugi-covered region near the Italian Antarctic base, also in the Terra Nova Bay area. They found the total albedo to be between 0.75 in the morning and 0.90 in the evening. They were able to explain this diurnal asymmetry with a geometrical sastrugi model. A similar geometrical sastrugi model was used by *Wendler and Kelley* (1988) to explain their asymmetrical diurnal cycle in albedo. They found total albedos for dry snow in the Terre Adelie ( $66^{\circ}S$ ,  $140^{\circ}E$ ) part of East Antarctica to be 0.83 for clear sky conditions and up to 0.90 for overcast conditions.

*Frezzotti et al.* (2002) have studied the effect of dunes and glazed areas on two traverses on the polar plateau of East Antarctica from Terra Nova Bay. They found that there is significant spectral variability in the albedo to distinguish glazed areas and dunes from each other and the surrounding snow. Glazing of snow occurs when accumulation has been negligible for a long period. Dunes form when the wind blows from the same direction persistently over many years.

*Grenfell et al.* (1994) made studies at the Amundsen-Scott South Pole station and at Vostok station ( $78^{\circ}27.85' S$ ,  $106^{\circ}51.95'E$ ). They found the spectral albedo of dry clean snow to have a uniformly high value of 0.96-0.98 across the ultraviolet (200 to 400 nm) and visible (400 to 850 nm) spectra, and to be nearly independent of snow grain size or solar elevation. In the near infra-red (850 to 3000 nm), they found the albedo to be lower, dropping to below 0.15 in the strong absorption bands at 1500 and 2000 nm. Some of the spectra in the present study show lower values than these. These differences can be due to the much smaller grains found high on the polar plateau where

there is constant precipitation in the form of very small snow grains called diamond dust. The measured higher values in the present study were obtained under an overcast sky.

## 5. *Conclusions*

Measurements of total albedo and spectral albedo (in the waveband 300-1100 nm) over snow and blue ice, together with some snow surface properties, were made during two austral summers in the Dronning Maud Land region of Antarctica. In 1999/2000, the measurements were made along a traverse going inland from the coast via the Finnish Antarctic research station Aboa and in 2000/2001 at the South African station SANAE 4. The following conclusions can be made from the results.

1) In addition to providing more spectral albedo data for the Dronning Maud Land region of Antarctica, and especially the region surrounding SANAE 4, the results give a better idea of how small the spatial variability of the albedo is and how the ambient conditions are of great importance.

2) The mean spectral albedos for snow from the Aboa transect and from SANAE 4 were statistically similar. They showed values of 0.95 in the visible band with very little dependence on wavelength. After 700 nm, the wavelength dependence increased and at 1034 nm, the albedos dipped to 0.70. The spectral albedos were similar in magnitude or only slightly lower than values obtained in the South Pole region.

3) Blue ice spectral albedos from the different areas showed a larger variability. The maxima were between 0.80 and 0.92, at 400 nm, and the minima were between 0.10 and 0.46, at 1034 nm.

4) Midday total albedo values were between 0.85 and 0.90 for snow for overcast conditions. Some diurnal variations were found with the lowest albedos being in the mornings and in the evenings. The total albedos obtained were slightly higher than values obtained in other studies in the Dronning Maud Land region but very similar to values obtained at the South Pole.

5) The narrowband albedo in the 700-3000 nm band was found to depend on the total albedo with a coefficient of determination of 0.71. The ultraviolet albedo was found to depend on the narrowband albedo in the 700-3000 nm band with a coefficient of determination of 0.85.

6) Using Landsat Thematic Mapper band ratios, surfaces could be classified into snow and blue ice. The classification boundaries are [0.90, 0.98] for snow and [0.33, 0.76] for blue ice. The dependence of this band ratio on the solar angle was very weak for both blue ice and snow. More measurements of superimposed ice are needed to make a better classification of different surface types.

## 6. *Acknowledgements*

This study was funded by the Academy of Finland through the project "Seasonal Snow in Antarctica" (SA43925). Further assistance was received from the South

African National Antarctic Programme (SANAP) and the Finnish Antarctic Research Programme (FINNARP) are acknowledged for making this research possible. Matti Leppäranta is acknowledged for his help in preparing this manuscript. Three anonymous referees are acknowledged for their patience in reading the manuscript and making constructive comments.

### *References*

- Bintanja, R., 1999. On the glaciological, meteorological and climatological significance of Antarctic blue ice areas, *Reviews of Geophysics*, **37**, 337-359.
- Bintanja, R. and M. Van den Broeke, 1995. The surface energy balance of Antarctic snow and blue ice, *J. Appl. Meteor.*, **34**, 902-926.
- Carroll, J.J. and B.W. Fitch, 1981. Effects of solar elevation and cloudiness on snow albedo at the South Pole, *J. Geoph. Res.*, **86**, 5271-5276.
- Casacchia, R., R. Salvatori, A. Cagnati, M. Valt and S. Ghergo, 2002. Field reflectance of snow/ice covers at Terra Nova Bay, Antarctica, *Int. J. Rem. Sens.* **23**, 4653-4667.
- Frezzotti, M., S. Gandolfi, F. La Marc and S. Urbini, 2002. Snow dunes and glazed surfaces in Antarctica: new field and remote-sensing data, *Ann. Glaciol.* **34**, 81-88.
- Gay, M., M. Fily, C. Genthon, M. Frezzotti, H. Oerter and J.-G. Winther, 2002. Snow grain-size measurements in Antarctica, *J. Glaciol.*, **46**, 27-535.
- Grenfell, T.C., S.G. Warren and P.C. Mullen, 1994. Reflection of solar radiation by the Antarctic snow surface at ultraviolet, visible, and near-infrared wavelengths, *J. Geophys. Res.*, **99**, 18669-18684.
- Grenfell, T.C and D.K. Perovich, 2004. Seasonal and spatial evolution of albedo in a snow-ice-land-ocean environment, *J. Geophys. Res.*, **109**, C01001, doi:10.1029/2003JC001866.
- Greuell, W., C.H. Reijmer and J. Oerlemans, 2002. Narrowband-to-broadband albedo conversion for glacier ice and snow based on aircraft and near-surface measurements, *Remote Sensing of Environment*, **82**, 48-63.
- Hoinkes, H.C., 1961. Studies of solar radiation and albedo in the Antarctic, *Arch. Meteorol. Geophys. Bioklimatol.* **B10**, 175-181.
- Kärkäs, E., H.B. Granberg, K. Kanto, K. Rasmus, C. Lavoie and M. Leppäranta, 2002. Physical properties of the seasonal snow cover in Dronning Maud Land, East-Antarctica, *Ann. Glaciol.*, **34**, 89-94.
- Kärkäs, E., T. Martma and E. Sonninen, 2005. Physical properties and stratigraphy of surface snow in Western Dronning Maud Land, Antarctica, *Polar Research*, **24**, 55-67.
- Liljequist, G.H., 1956. Energy exchange of an Antarctic snow-field. Shortwave radiation (Maudheim 71°03'S, 10°56'W). Norwegian-British-Swedish Antarctic Expedition, 1949-52. Sci. Results II, Part 1A, 1-109.

- Mishra, V.D., 1999. Albedo variations and surface energy balance in different snow-ice media in Antarctica, *Defence Science Journal*, **49**, 347-362.
- Orsini, A., F. Calzolari, T. Georgiadis, V. Levizzani, M. Nardino, R. Pirazzini, R. Rizzi, R. Sozzi and C. Tomasi, 2000. Parameterisation of surface radiation flux at an Antarctic site, *Atmospheric Research*, **54**, 245-261.
- Pirazzini, R., 2004. Surface albedo measurements over Antarctic sites in summer, *J. Geophys. Res.*, **109**, D20118, doi: 10.1029/2004JD004617.
- Reijmer, C.H., R. Bintanja and W. Greuell, 2001. Surface albedo measurements over snow and blue ice in thematic mapper bands 2 and 4 in Dronning Maud Land, Antarctica, *J. Geophys. Res.*, **106**, 9661-9672.
- Van den Broeke, M., 2004. On the role of Antarctica as heat sink for the global atmosphere, *Journal de Physique IV*, **121**, 115-124.
- Van den Broeke, M.R., J.-G. Winther, E. Isaksson, J.F. Pinglot, L. Karlöf, T. Eiken and L. Conrads, 1999. Climate variables along a traverse line in Dronning Maud Land, East Antarctica, *J. Glaciol.*, **45**, 295-302.
- Warren, S.G., 1982. Optical properties of snow, *Rev. Geophys. Space Phys.*, **20**, 67-89.
- Warren, S.G. and A.D. Clarke, 1990. Soot in the atmosphere and snow surface of Antarctica, *J. Geophys. Res.*, **95**, 1811-1816.
- Wendler, G. and J. Kelley, 1988. On the albedo of snow in Antarctica: a contribution to I.A.G.O., *J. Glaciol.*, **34**, 19-25.
- Wiscombe, W.J. and S.G. Warren, 1980. A Model for the Spectral Albedo of Snow, I: Pure Snow, *J. Atmosph. Sci.*, **37**, 2712-2733.